International Journal of Micro Air Vehicles

Article

International Journal of Micro Air Vehicles
0(0) 1–10

DOI: 10.1177/1756829318771059
journals.sagepub.com/home/mav
SAGE

The choice of sliding surface for robust roll control: Better suppression of high angle of attack/sideslip perturbations

S Seyedtabaii and M Delavari

Abstract

The nominal aerodynamic parameters of aircraft are often approximate and aircraft may experience high value of angle of attack/sideslip perturbations during their manoeuvres. Preventing instability and air crash requires a robust controller capable of containing the dynamic uncertainty and the perturbations. In this respect, the problems of roll control in such a situation are studied and a better choice of sliding surface is proposed. Sliding mode control manages the uncertainty and adaptive fuzzy is employed to shape the transient response. As a result, a setup is formed which outperforms the basic controller both in terms of transient speed, response robustness and control effort. The strength of the method is more appreciated in case of high angle of attack/sideslip perturbed manoeuvres. This is proved theoretically and illustrated by simulations.

Keywords

Flight control, high angle of attack, adaptive fuzzy sliding mode, roll stabilization

Received 22 July 2017; accepted 30 January 2018

Introduction

The aim of an aircraft control loop is to enforce accurate tracking of the ordered lateral-directional and longitudinal commands in all intended flight manoeuvres over a wide range of working conditions. A well-tuned feedback control law is expected to suppress external disturbances (e.g. wind gusts) and to reduce sensitivity to the aircraft parameters' variations (robustness against parametric uncertainties).

Design of an aircraft control is tough due to nonlinearity, coupling and time varying characteristics of the system[1] and strong dependency of the system parameters to the working conditions, i.e. angle of attack/sideslip. Nevertheless, gain scheduling (GS) approach is traditionally employed where the system dynamic around each axis is linearized and the proportional-integral-derivative (PID) controller is independently utilized for each axis. Success of the design depends on the precise definition of the type of operation so that the neglected dynamic and cross-couplings among variables to be adequately small. Apart from that, a lot of more sophisticated approaches such as: fuzzy logic (FL),[2] intelligently tuned μ-PID,[3] robust,[4] intelligently tuned fractional order PID,[5] sliding mode,[6] H∞, fractional order PID,[7] dynamic inversion, a combination of model inversion with an online adaptive neural network, a nonlinear adaptive design based on backstepping, neural networks and RBFNN-based adaptive design[8] have also been studied. The main goal in all of the newly developed methods is flight envelope extension and manoeuvrability improvement.

Sliding mode control (SMC) has been commonly used in aerospace,[6] process control, power control and robotics to administer dynamic and disturbance perturbations. However, SMC results in a high switching gain particularly when the system uncertainty band is large. This may cause degradation of the steady-state performance and system failure due to mechanical

Electrical Engineering Department, Shahed University, Tehran, Iran

Corresponding author:
S Seyedtabaii, Electrical Engineering Department, Shahed University, Tehran, Iran.
Email: stabaii@shahed.ac.ir

vibrations. The problem has well been investigated,[9,10] and modifications have been developed, e.g. instead of using fixed switching gain, various adaptive nonlinear gain algorithms have been introduced.[11,12] By integrating adaptive fuzzy and SMC, various types of interesting methods are formed.[13] In Amieur et al.,[14] adaptive fuzzy SMC (AFSMC) alongside with feedback linearization has been explored. Application of AFSMC for a flexible robot[15] and a hypersonic vehicle control has also been reported.[16] For a simplified F/A-18 aircraft model, a nonlinear AFSC is designed for trajectory tracking during aircraft manoeuvres.[17] Application of integral back stepping SMC has also been elaborated in Jia et al.[18] In Su et al.,[19] a combined backstepping and dynamic surface control for adaptive fuzzy-state feedback control has been investigated. A novel adaptive fuzzy gain-scheduling sliding mode control (AFGS-SMC) method for attitude regulation has been addressed in Yang et al.[20] Adaptive fuzzy multi-surface sliding control (AFMSSC) for trajectory tracking of an MIMO aerial vehicle has been detailed in Norton et al.[21] In Rubagotti et al.,[22] integral sliding mode controller for reducing disturbances is the subject of study. A nonlinear sliding mode controller using bifurcation for commanded spin of an aircraft is given in Rao and Sinha.[23] Employing robust SMC approach to deal with nonlinear uncertain behavior of actuator of micro aerial vehicles (MAV) are the subject of investigation in Guruganesh et al.[24] Adaptive sliding control law for managing the atmospheric environment of Mars airplane is detailed in Liu et al.[25]

In this paper, the uncertainty in the aerodynamic parameters of an aircraft and its negative influences on an already designed roll controller are investigated. It is shown that in a low angle of attack/sideslip manoeuvring, the effect of uncertainty is almost entirely confined by the basic controller. However, this is not true when the vehicle is thrown into a high angle of attack/sideslip conditions by known or unknown disturbances. A type of condition realized that it might end up in the so-called unstable falling leaf motion. In this respect, by appreciating the past investigations, a modified sliding surface by a weighted combination of roll rate, p, and sideslip angle, β is introduced which yields better transient response at lower control effort. The performance is more improved when SMC is modified to a special AFSMC configuration. It is shown that the method is capable of providing safe and reliable flight motion in spite of 30% tolerances in the aircraft roll aerodynamic parameters and against high value of angle of attack/sideslip perturbations. This is proved theoretically and illustrated through extensive simulations.

The paper table of contents is as follows:

- Aircraft control: Equation of motion, Aircraft control, Roll aerodynamic uncertainty.
- Robust roll FSMC control: SMC design, Adaptive k using adaptive fuzzy algorithm.
- Simulations
- Conclusion

Aircraft control

Generally, longitudinal and lateral-directional motion of an aircraft is governed by the three main control urfaces: elevators, rudders and ailerons. Longitudinal or pitch axis control is directed by the symmetric deflection of the elevators. Deflection of the ailerons manages the roll, and the lateral-direction (yaw) motion is managed by the joint rudder-aileron action.

Equations of motion

The six-degrees of freedom nine-state mathematical model of an aircraft are expressed in a nonlinear state space form as follows

$$\dot{x} = f(x, u)$$

where $x = [V, \beta, \alpha, p, q, r, \phi, \theta, \psi]$ is a vector of nine states, i.e. speed, sideslip angle, angle of attack, roll rate, pitch rate, yaw rate, roll angle, pitch angle and yaw angle, respectively. The functioning of the control surfaces is expressed in the vehicle dynamics equations by $u = [\delta_a, \delta_r, \delta_s]$ which is a vector of three control surfaces angles. The aircraft force equations[1] are given by

$$\begin{aligned}
\dot{V} &= \frac{1}{m}(-D\cos\beta + Y\sin\beta + T\cos\alpha\cos\beta) \\
&\quad + g(-\cos\alpha\cos\beta\sin\theta + \sin\beta\cos\theta\sin\varphi + \sin\alpha\cos\beta\cos\theta\cos\varphi) \\
\dot{\alpha} &= q + \frac{1}{mV\cos\beta}(-L - T\sin\alpha + mg(\cos\beta s\varphi\cos\theta + \sin\alpha\sin\theta) \\
&\quad -\tan\beta(p\cos\alpha + r\sin\alpha)) \\
\dot{\beta} &= \frac{1}{mV}(Y\cos\beta + D\sin\beta - T\sin\beta\cos\alpha) + p\sin\alpha - r\cos\alpha \\
&\quad + \frac{g}{V}(\cos\beta\cos\theta\sin\varphi + \cos\alpha\sin\theta\sin\beta - \sin\alpha\cos\theta\cos\varphi\sin\beta) \\
D &= C_D^{\alpha}(\beta, \delta_{Stab}), \quad L = C_L^{\alpha}(\beta, \delta_{Stab}), \\
Y &= C_Y^{\alpha}(\beta, \delta_{ail,}\delta_{rud})
\end{aligned} \tag{1}$$

where D, L, Y and T are the drag, lift, side and trust forces. The Euler angles rates are also

formulated by

$$\begin{bmatrix} \dot{\varphi} \\ \dot{\theta} \\ \dot{\psi} \end{bmatrix} = \begin{bmatrix} 1 & \sin\varphi\tan\theta & \cos\theta\tan\theta \\ 0 & \cos\varphi & -\sin\varphi \\ 0 & \sin\varphi/\cos\theta & \cos\varphi/\cos\theta \end{bmatrix} \begin{bmatrix} p \\ q \\ r \end{bmatrix}$$

The three moment equations which are directly related to the aerodynamic parameters are given below[1]

$$\begin{aligned} \dot{p} &= kI_{zz}C_l + kI_{xz}C_n + I_{yy}qr + I_{xz}pq - I_{zz}rq \\ \dot{q} &= \frac{0.5\rho V^2 S\overline{c}}{I_{yy}} C_m - I_{xx}pr + I_{xz}r^2 - I_{xz}p^2 + I_{zz}rp \\ \dot{r} &= kI_{xz}C_l + kI_{xx}C_n + I_{zz}pq - I_{xz}rq - I_{yy}qp \end{aligned}$$

$$\mathrm{k} = \frac{0.5\rho V^2 Sb}{(I_{xx}I_{zz} - I_{xz}^2)}, \qquad C = \begin{bmatrix} C_l^{\alpha,V}(\beta, \delta_{ail,}\delta_{rud,}p, r) \\ C_m^{\alpha,V}(\delta_{stab,}q) \\ C_n^{\alpha,V}(\beta, \delta_{ail,}\delta_{rud,}p, r) \end{bmatrix} \tag{2}$$

Some of the system parameters taken from the F/A-18 fighter airplane have been depicted in Table 1. The other parameters involved are C_l, C_m and C_n which are aerodynamic roll, pitch and yaw coefficients, respectively. These parameters are nonlinear functions of the system variables and often vary as flight condition changes.

Considering the nonlinear dynamical equations (1) and (2), significant coupling among roll and yaw and sideslip is noticed and the model contains most of the nonlinear characteristics of the system to be used for unstable mode simulations.

For the purpose of control design, the aerodynamic coefficients, mainly derived experimentally, are stated in terms of approximate polynomial equations such as the one for C_l as below[1]

$$\begin{aligned} C_l = {} & \left(-1.619\alpha^4 + 2.3843\alpha^3 - 0.3620\alpha^2 - 0.4153\alpha - 0.0556\right)\beta \\ & + \left(0.9189\alpha^3 - 0.2646\alpha^2 - 0.0516\alpha + 0.1424\right)\delta_{ail} \\ & + \left(-0.027\alpha^3 + 0.0083\alpha^2 + 0.00416\alpha + 0.0129\right)\delta_{rud} \\ & + \frac{37.42}{2V}(-1.0871\alpha^2 + 0.7804\alpha + 0.1983)r \\ & + \frac{37.42}{2V}(0.2377\alpha - 0.3540)p \end{aligned} \tag{3}$$

By substituting C_l in $\dot{p}$ (equation (1)), the roll rate nominal equation is obtained as follows

$$\begin{aligned} \dot{p} = {} & (0.0317q + V(0.0016\alpha - 0.0023))p \\ & + \left(-0.8151q + V\left(-0.0071\alpha^2 + 0.0051\alpha + 0.0013\right)\right)r \\ & + 10^{-4}V^2(-5.6310\alpha^4 + 8.2890\alpha^3 - 1.2350\alpha^2\beta \\ & - 1.4460\alpha - 0.19800) \\ & + 10^{-5}V^2(6.7510\alpha^3 - 8.9920\alpha^2 - 1.8360\alpha \\ & + 49510)\delta_{ail} \\ & + 10^{-6}V^2(-2.37\alpha^4 - 4.068\alpha^3 - 0.497\alpha^2 + 0.594\alpha \\ & + 4.959)\delta_{rud} \end{aligned} \tag{4}$$

$\dot{p}$ (4) can be expressed in a compact form by

$$\begin{aligned} \dot{p} = {} & 0.0317qp - 0.8151qr + K_p(\alpha)p \\ & + K_r(\alpha)r + K_\beta(\alpha)\beta + K_{ail}(\alpha)\delta_{\mathrm{ail}} + K_{rud}(\alpha)\delta_{\mathrm{rud}} \end{aligned} \tag{5}$$

This is one of the nine equations stating the nonlinear, coupled and time varying (due to change in mass and v) behaviour of the simulated system. Any designed controller is expected to be able to offer stable and safe flight considering the family of the equations similar to equation (5).

Table 1. Aircraft parameters.[1]

Parameter	Symbol	Value
Wing area	S	37.16 m^2
Wing span	b	11.4 m
Mean aerodynamic chord	$\overline{c}$	3.51 m
Mass	m	15,097.4 kg
Roll axis moment of inertia	Ixx	31,183 $kg.m^2$
Pitch axis moment of inertia	Iyy	205,125 $kg.m^2$
Yaw axis moment of inertia	Izz	230,414 $kg.m^2$
Cross product of inertia about y axis	Ixz	−4028 $kg.m^2$
gravitational constant	g	9.8 m/s^2
Air density at 25°C and 7625 m	ρ	0.55kg/m^3
Thrust	T	645,000 N
Air speed	V	106.5 m/s

Aircraft control

The simplified basic flight control of the F/A-18 aircraft is as follows[1]

$$\begin{aligned} \delta_{elev} &= (8q + 0.8\alpha)G_A(s) \\ \delta_{rud} &= \left(0.5a_y + \frac{1.1s + 6}{s + 1}r\right)G_A(s) \\ \delta_{ail} &= \left(-0.8p - 0.5\beta - 2\dot{\beta}\right)G_A(s) \end{aligned}$$

where the actuator, $G_A(s)$ is modelled by a first-order lag. For the longitudinal control, α and q are measured

and used for stabilization. The directional control consists of feedback from yaw rate, r and lateral acceleration $\alpha_y = f(C_Y)$ to the rudder actuator. The lateral acceleration feedback aims at reducing sideslip during coordinated turn.[26] Initially, for the roll control just a p feedback, $\delta_{ail} = -0.5p$, was used, and the values of the controller parameters were validated by performing numerous simulations.[1]

Later on, due to several high angle of attack perturbation related air crashes,it is realized that the controller is not qualified for stopping the so-called unstable falling leaf motion, a type of out of control action with a large coupled oscillations in p and r along with substantial fluctuations in α and β.[1] During large angle-of-attack/sideslip motion, the dihedral effect (roll caused by sideslip) of the aircraft wings becomes extremely large and the directional stability becomes unstable.[1] Therefore, to manage the instability, the basic control law

$$\delta_{ail} = -0.8p - 0.5\beta - 2\dot{\beta}$$

was suggested and employed that augments the roll feedback with two extra β and $\dot{\beta}$ loops. By this, the control action is calculated in a way that not only p is stabilized, but also to damp both β and $\dot{\beta}$.

Further investigations in improving the response of the aircraft in facing falling leaf, led to the control signal

$$U_{ail} = -1.4p - 18\beta - 8\dot{\beta} - \frac{0.584}{s+1}r$$

containing an extra heading rate loop that it is shown to be more effective than the basic one.[27]

Roll aerodynamic uncertainty

It is natural to assume approximation in the values of the parameters of equation (1). For roll control, the engaged equation is

$$\dot{p} = kI_{zz}C'_l + kI_{xz}C'_n + I_{yy}qr + I_{xz}pq - I_{zz}rq$$

where C'_l and C'_n are the uncertain C_l and C_n. The equation may be short written as follows

$$\dot{p} = K_p(\alpha)p + K_\beta(\alpha)\beta + K_{ail}(\alpha)\delta_{\text{ail}} + \text{d}(.)$$
$$d(.) = 0.0317qp - 0.8151qr + + K_r(\alpha)r + K_{rud}(\alpha)\delta_{\text{rud}} \quad (6)$$

To model the uncertainty for the simulation purpose, a family of random systems may be generated using either of the following two approaches. In the first method, randomness is applied to the aerodynamic parameters of equation (3) (and similarly to the parameters of C_n) which consequently renders a set of random $\dot{p}$ (6) equations. The effect of C_m uncertainty in $\dot{p}$ is around 2% when compared with C_l uncertainty. To illustrate the effect of uncertainty on the parameters of equation (6), K_{ail} and K_β versus α have been presented in Figure 1(a) and (b) where α ranges from -0.5 to 1.5 radians. To produce realistic random systems, $k_{ail}>0$ and $K_\beta<0$ constraints have also been applied. As the figures indicate, 10% variation in the coefficients leads to drastic large tolerances at higher α values. Alternatively, the uncertainty may be applied directly to the parameters of equation (6) instead of equation (3) which yield more realistic random systems. The result of applying 30% uncertainty to the K parameters of equation (6) has been shown in Figure 1(c) and (d) which looks more appropriate for the uncertainty evaluations.

Now, the prime question here is that how any randomness in the parameters of equation (6) alters the roll response and flight performance. As the figures indicate, in low angle of attack, there might be no significant operation degradation, but it may not be true when the aircraft is entangled with a high angle of attack perturbations.

Robust roll FSMC control

In our simulations, it is shown that the basic control law fails in securing flight performance in face of tolerances in the p parameters (equation (6)) when the vehicle experiences some high angle of attack/sideslip perturbations. Hence, modifications to the controller or a new controller are required. For combating dynamic uncertainty, SMC is a controller of choice that cannot be ignored particularly when the size of ambiguity is supposedly unknown and large.

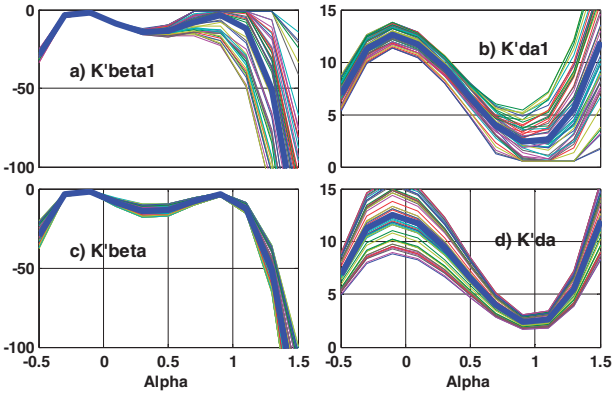

Figure 1. Uncertain K_β and $K_{\delta ail}$ parameters of $\dot{p}$ (6). (a) K'beta1, (b) K'da1, (c) K'beta and (d) K'da.

The block diagram of the proposed adaptive fuzzy sliding mode controller is shown in Figure 2, which consists of the system, sliding mode controller, fuzzy system and adaptive algorithm.

SMC design

To start with SMC control design,[20,21] the past investigations leading to the basic control law is appreciated and a new variable, z is introduced by a weighted combination of p and β as follows

$$z = p + w\beta \tag{7}$$

The dynamic equation of the new variable is composed by employing $\dot{p}$ from equation (6) and $\dot{\beta}$ from equation (1). Considering the uncertainty in equation (6) and cross-coupling among variables, the dynamic of z is given by

$$\dot{z} = \underline{a}z + \underline{b}\delta_{ail} + \underline{\Delta} + d(.), \qquad |d(.)| < \delta \tag{8}$$

where $\underline{\alpha}$, $\underline{b}$ and $\underline{\Delta}$ are the nominal values and δ is an scalar sufficiently large lumped bound for the dynamic uncertainty, $d(.)$.

Remarks

The uncertainty is only applied to the roll-related aerodynamic parameters C_l and C_n and the other aerodynamic parameters attain their nominal values.

Assumptions:

1. The basic controller stabilizes the states with nominal parameters including sideslip.[1]
2. The initial conditions are within the region of attraction of the basic control law.[1]

Other than the $\underline{a}w\beta$ term, the rest of the $w\dot{\beta}$ dynamics are collected in $\underline{\Delta}$ since uncertainty is only going to be applied to the roll parameters (Remark 1), otherwise the rudder and elevator controls have to be modified similarly.

Note that the stability of β directed by the nominal system rudder closed loop control (Remark 2); the asymptotical stability of p is definite if a control action forces to zero the tracking error function

$$e = z - z_0 = p - p_{trim} + w(\beta - \beta_{trim}) \tag{9}$$

in response to any perturbation. In this respect, the following integral sliding surface

$$s = e + \lambda \int e(t)\mathrm{d}t \tag{10}$$

is introduced. The system enjoys asymptotic stability if the control action, δ_{ail} makes the derivative of the quadratic Lyapunov function $V(s) = s^2/2$ negative definite as below

$$\dot{V}(s) = s\dot{s} \prec 0$$

To develop such a stabilizer, under constant trim condition, $\dot{s}$ is calculated

$$\dot{s} = \dot{e} + \lambda e = 0 \quad for \quad t > 0 \tag{11}$$

The aileron control signal stabilizing the nominal system using feedback linearization is obtained as follows

$$u_{eq} = -\underline{b}^{-1}\left(\underline{a}e + \underline{\Delta} + \widehat{d} + \lambda e\right) \tag{12}$$

if the bound on the aileron deflection is not violated. $\widehat{d}$ is an ad hoc estimate of d if it is available, otherwise $\widehat{d} = 0$. In case of parameter uncertainty and inaccurate estimate of d, equation (12) is not adequate and as usual of SMC a switching control is needed to handle the parameter uncertainty and to push s toward the sliding surface. It is enforced by

$$u_{sw} = -k\underline{b}^{-1}\mathrm{sgn}(s) \tag{13}$$

Applying both continuous and switching control law to the system results in

$$\begin{aligned} \dot{V} &= s\dot{s} = s(\underline{a}e + \underline{b}u_{eq} + \underline{b}u_{sw} + \underline{\Delta} + d + \lambda e) \\ &\leq s(-\underline{b}k\underline{b}^{-1}\mathrm{sgn}(s) + d - \widehat{d}) < 0 \end{aligned} \tag{14}$$

Equation (14) is negative definite and asymptotical stability is ensured for adequately large k if the

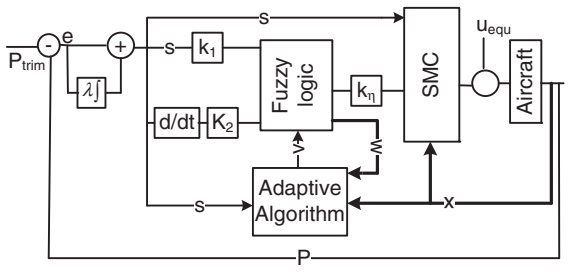

Figure 2. Block diagram of the adaptive fuzzy sliding mode controller.
SMC: sliding mode control.

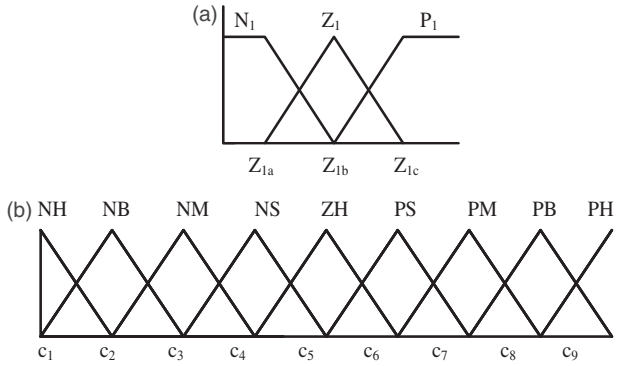

Figure 3. Membership functions of (a) s and ṡand (b) $\widehat{d}$.

following conditions are met

$$\underline{b}\pm\delta_b > 0, \quad \delta_{ail-LB} < u_{eq} + u_{sw} < \delta_{ail-UB}$$
$$k > |d - \widehat{d}\,| + \eta \tag{15}$$

where η is a positive constant. It is a common practice to replace the switching operator of the discontinuous control action with the saturation function to mitigate its adverse effects as follows

$$\begin{aligned}\delta_{ail} &= u_{eq} + u_{sw} \\ &= -\underline{b}^{-1}\left(\underline{a}z + \underline{\Delta} + \widehat{d} + \lambda e + k \times sat\left(\tfrac{s}{\hat{a}}\right)\right)\end{aligned} \tag{16}$$

here $\hat{a}$ is an appropriate small constant.

Adaptive k using adaptive fuzzy algorithm

The problem of SMC chattering is relatively mitigated by using saturation instead of switching (equation (16)). However, better performance is also expected if adaptive k is used by estimating $\widehat{d}$, alternatively. The latter can be applied using fuzzy techniques.

The inputs to the fuzzy system are sliding surface, s and its derivative, $\dot{s}$. Each of the inputs is fuzzified through a three-membership function fuzzifier, Figure 3(a). The output, defuzzifier, is composed of a nine-membership function set with adaptable membership functions centres, c_1 to c_9, Figure 3(b).

A set of nine rules composes the fuzzy inference rule bank, shown in Table 2. They are formed using the following abbreviations:

N: Negative; Z: Zero and P: Positive
H: Huge; B: Big; M: medium; S: Small

The k_1, k_2 and $K_{\widehat{d}}$ parameters are the fuzzy scaling factors, Figure 3. The defuzzification process is

Table 2. The fuzzy inference rules.

		$\dot{\sigma}$		
		P	**Z**	**N**
s	**P**	NH	NB	NM
	Z	NS	ZE	PS
	N	PM	PB	PH

conducted using the centre of area method (COA) which is expressed by the following equation

$$\begin{aligned}\widehat{v} &= \begin{bmatrix}\widehat{c}_1 \\ \dots \\ \widehat{c}_9\end{bmatrix}, W = \frac{1}{\sum_{i=1}^{9} w_i}\begin{bmatrix}w_1 \\ \dots \\ w_9\end{bmatrix} \Rightarrow \widehat{d} = \frac{\sum_{i=1}^{9} w_i c_i}{\sum_{i=1}^{9} w_i} \\ &= \widehat{\nu}^{\,T} W(s, \dot{s})\end{aligned}$$

where $\widehat{c}_1$ to $\widehat{c}_9$ are the estimates of the centre of $\widehat{d}$ membership functions and W is a vector of degree of membership to each of the nine $\widehat{d}$ membership functions.

Let $\widehat{d}^* = \widehat{v}^* W$ be an optimum value for the uncertainty, d, where $\widehat{v}^*$ is its associated optimal parameter. The adaptive fuzzy estimator is expected to minimize $\widehat{d} - \widehat{d}^*$ distance or alternatively $e = \widehat{v} - \widehat{v}^*$ adopting an appropriate adaptation law, while the overall system stability is also observed. This is ensured by employing the following two section positive definite Lyapunov functions[28]

$$V_T = \frac{1}{2}s^2 + \frac{1}{2\gamma}e^2, \quad e = \widehat{v} - \widehat{v}^{\,*}$$

where γ is a positive constant. Taking the time derivative of V_T and using equation (14) yields

$$\begin{aligned}\dot{V}_T &= s\dot{s} + \frac{1}{\gamma}\dot{e}e = \\ &= s(\underline{a}e + \underline{b}u_{eq} + \underline{b}u_{sw} + \underline{\Delta} + d - \widehat{d}^{\,*} + \widehat{d}^{\,*} + \lambda e) \\ &\quad + \frac{1}{\gamma}\dot{e}e\end{aligned}$$

Now, by using equations (12) and (13), the following results are obtained

$$\begin{aligned}\dot{V}_T &= s(-\underline{b}k\underline{b}^{-1}\mathrm{sgn}(s) + d - \widehat{d}^{\,*} + \widehat{d}^{\,*} - \widehat{d}\,) + \frac{1}{\gamma}\dot{e}e \\ &= s(-\underline{b}k\underline{b}^{-1}\mathrm{sgn}(s) + d - \widehat{d}^{\,*}) + esW(s, \dot{s}) + \frac{1}{\gamma}e\dot{e} \\ &= s(-\underline{b}k\underline{b}^{-1}\mathrm{sgn}(s) + \rho) + \frac{1}{\gamma}e(\dot{e} + \gamma sW(s, \dot{s}))\end{aligned} \tag{17}$$

Next, by adopting the adaptation law

$$\dot{e} = -\gamma sW(s, \dot{s}) \Rightarrow \dot{v} = -\gamma sW(s, \dot{s})$$

the second part of equation (17) is crossed out and it is reduced to

$$\dot{V}_T = s(-\underline{b}k\underline{b}^{-1}\mathrm{sgn}(s) + \rho) \leq -\eta|s|$$

where more mild condition for k than equation (15) is reached as below

$$|d - \hat{d}| + \eta > k > \rho + \eta > |d - \hat{d}^*| + \eta$$

The γ parameter is related to the adaptation rate. By this provision, the level of switch control is no longer constant but depends on the error values defined by s and $\dot{s}$.

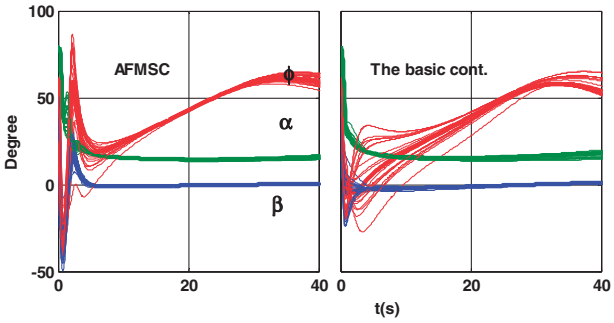

Figure 4. The performance of AFSMC (left) and the basic controller (right) in stabilizing the family of random systems against high α and β perturbations in a non-realistic simulation (no limit on the aileron deflection angle).
AFSMC: adaptive fuzzy sliding mode control.

Simulations

The system (equation (1)) is simulated using parameters depicted in Table 1 and aerodynamic parameters reported in Chakraborty et al.[1] Apart from the nominal system, a family of 50 randomly generated systems with 30% tolerance in the K^* parameters of equation (6) is produced.

The performance of the basic and the proposed AFSM controllers are evaluated in maintaining reliable and secure flight operation in spite of the aerodynamic parameter uncertainty under high angle of attack/sideslip perturbations. The basic controller can handle system uncertainty well under low angle of attack flight running. However, in facing a type of manoeuvre reported in Chakraborty et al.,[1] which may lead to falling leaf instability, serious problems occur. One of such operations occurs under the following working point (trim values)

$$x = [\,V \quad \beta \quad \alpha \quad p \quad q \quad r \quad \varphi \quad \theta \quad \psi\,]^T$$
$$x_{Trim} = [\,106.5 \quad 0 \quad 20 \quad -1 \quad 2 \quad 2.5 \quad 35 \quad 19 \quad 0\,]^T$$

Four sets of initial condition perturbations are considered (Remark 3). The first one is a high angle of attack and sideslip perturbation given by the following vector

$$x_{Initial} = [\,106.5 \quad 50 \quad 80 \quad 24 \quad 2 \quad 3 \quad 60 \quad 19 \quad 0\,]^T$$

First, a nonrealistic simulation with no bound on the aileron deflection angle is performed. The responses of the two controllers have been presented in Figure 4. The AFSMC parameters are $w = 4$ and $\lambda = 2$. As it is noted from the graphs, the proposed controller

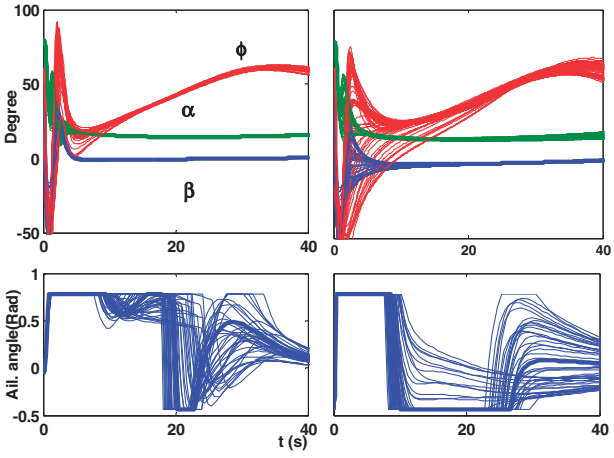

Figure 5. The performance of AFSMC (left) and the basic controller (right) in stabilizing the family of random systems against high α and β perturbations.

stables the system faster with lower control effort than what the basic controller demands.

Imposing a bound on the aileron deflection ($-25°$ to $45°$)[1] and repeating the test under similar conditions render performances portrayed in Figure 5. Faster response and more coherent behavior, which is expected from a well-designed robust controller, is achieved For the sake of conciseness, the other stable states are not shown.

The superiority of using z instead of p in forming the sliding surface has been illustrated in Figure 6. By using $w = 0$, the sliding surface based on $z = p$ is formed. The response of the system with $\lambda = 2$ has been depicted in Figure 6 (left). This shows how the system behaviour ends up in instability and flight failure. The same test is repeated with $\lambda = 0.1$ (slower convergence) by which the system stability is restored. Therefore, the

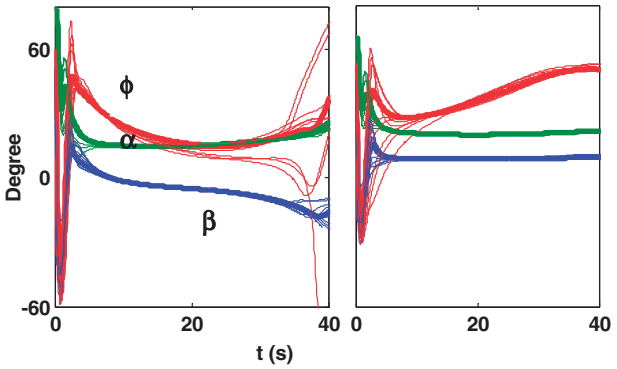

Figure 6. The AFSMC response with w = 0 and $\lambda = 2$ (left) and with w = 0 and $\lambda = 0.1$.

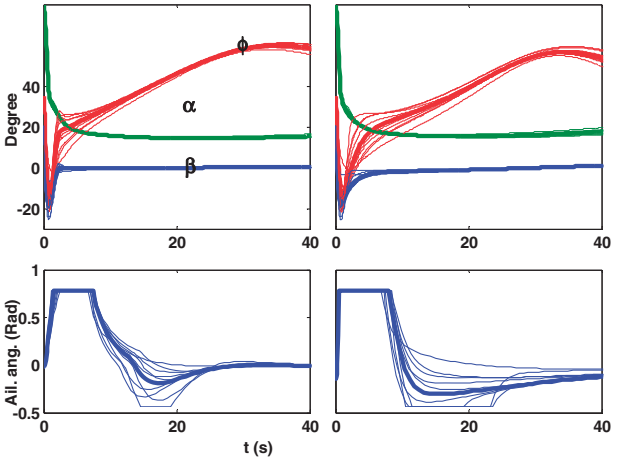

Figure 7. The performance of AFSMC (left) and the basic controller (RIGHT) in stabilizing the family of random systems against high α and medium β perturbations.

sliding surface based on z, yields faster transient response without stability compromise.

In the second test, the initial condition

$$x_{Initial} = [106.5 \quad 20 \quad 80 \quad 9 \quad 2 \quad 8 \quad 35 \quad 19 \quad 0]^T$$

is used in which the angle of attack initial condition is high, while the sideslip initial condition is medium. The performances of the AFSMC and the basic controller have been shown in Figure 7. The difference in coherency in the performance (robustness) is obvious from the figures plus faster transient response, the two advantages of the suggested controller against the basic one.

The third test is conducted under the following initial condition

$$x_{Initial} = [106.5 \quad 60 \quad 30 \quad 25 \quad 25 \quad 20 \quad 25 \quad 0 \quad 0]^T$$

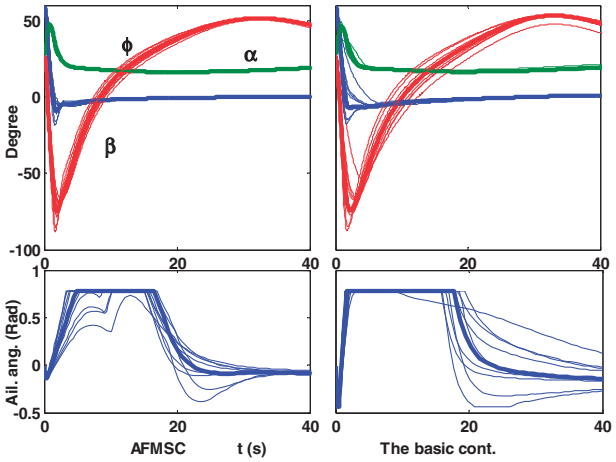

Figure 8. The performance of AFSMC (left) and the basic controller (right) in stabilizing the family of uncertain systems against medium α and high β perturbations.

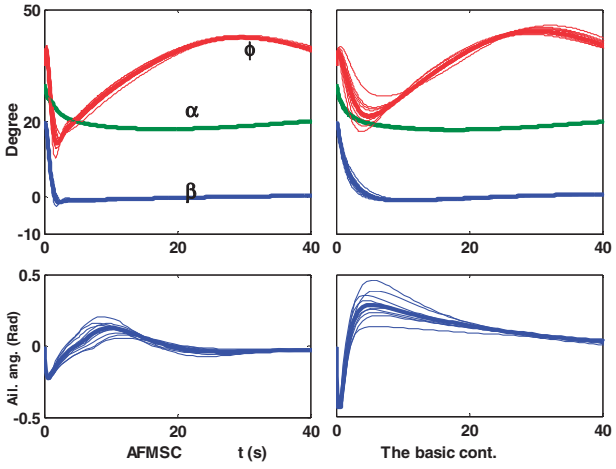

Figure 9. The performance of AFSMC (left) and the basic controller (right) in stabilizing the family of uncertain systems against medium α and β perturbations.

The results of the medium angle of attack and high sideslip perturbation are portrayed in Figure 8. Similar conclusions, i.e. faster transient and performance that is more robust are certified.

Eventually, the last test is conducted under the initial condition of

$$x_{Initial} = [106.5 \quad 20 \quad 30 \quad 30 \quad 20 \quad 3 \quad 35 \quad 10 \quad 0]^T$$

with medium angle of attack and sideslip angle perturbations. The results have been exhibited in Figure 9. Improvement in the response is projected in lower control effort needed for providing asymptotical stability.

The performance of the algorithm under other operating conditions within the region of attraction confirms the validity of the findings.

Conclusion

In this paper, the sensitivity of an aircraft roll control to the approximation in its aerodynamic parameters under high value of angle of attack and or sideslip perturbations are discussed. It is shown that at low values of perturbations, the performance of the already designed controller can be viewed acceptable and the flight performance is not degraded substantially. However, under high angle of attack/sideslip disturbances, like those that may end up in the falling leaf instability, the effect of approximation and uncertainty is substantial to the extent that it may cause air crash. In this respect, a novel sliding surface by a weighted combination of p and β is suggested. SMC is designed to contain the adverse effect of randomness in the system dynamic. The smoothness of the behaviour is managed by an adaptive fuzzy section that estimates the level of uncertainty and applies nonlinear switching control gain. As a result, the proposed controller enjoys performance that is more robust and delivers faster transient response with respect to the basic controller under various initial condition perturbations. This is proved theoretically and verified through extensive simulations.

Declaration of conflicting interests

The author(s) declared no potential conflicts of interest with respect to the research, authorship, and/or publication of this article.

Funding

The author(s) disclosed receipt of the following financial support for the research, authorship and/or publication of this article: This work has been partially supported by the research department of Shahed University.

ORCID iD

S Seyedtabaii http://orcid.org/0000-0001-7617-5542

References

1. Chakraborty A, Seiler P and Balas GJ. Susceptibility of f/a-18 flight controllers to the falling-leaf mode: linear analysis. *J Guid Control Dyn* 2011; 34: 57–72.
2. Babaei A, Mortazavi M and Moradi M. Classical and fuzzy-genetic autopilot design for unmanned aerial vehicles. *Appl Soft Comput* 2011; 11: 365–372.
3. Panahi H and Seyedtabaii S. Intelligently tuned μ-PID for aircraft lateral control. In: *2nd international conference on applied research in EMME*. Tehran, Iran, 18 Feb 2017.
4. Abdulhamitbilal E and Jafarov E. Robust sliding mode speed hold control system design for full nonlinear aircraft model with parameter uncertainties: a step beyond. In: *12th International Workshop on variable structure systems (VSS)*, IEEE, Bombay, India, 2012, pp.7–15.
5. Zaker S and Seyedtabaii S. On the performance of an intelligently tuned fractional order PID roll controller. In: *First international conference in applied research on EMME*, Tehran, Iran, 17 Feb. 2016.
6. Ali SU, Shah MZ and Samar R. Sliding mode based roll control law design for a research UAV and its flight validation. In: *13th international Bhurban conference on applied sciences and technology (IBCAST)*, IEEE, Islamabad, Pakistan, 2016, pp.118–125.
7. Seyedtabaii S. New flat phase margin fractional order PID design: perturbed UAV roll control study. *Rob Auton Syst* 2017; 96: 58–64.
8. Shin H and Kim Y. Flight envelope protection of aircraft using adaptive neural network and online linearisation. *Int J Syst Sci* 2016; 47: 868–885.
9. Edwards C and Spurgeon S. *Sliding mode control: theory and applications*. London, UK: Taylor & Francis, 1998.
10. Shtessel Y, Edwards C, Fridman L, et al. *Sliding mode control and observation*. New York: Springer, 2014.
11. Hu X, Wu L, Si X, et al. Adaptive sliding mode control of non-linear non-minimum phase system with input delay. *IET Control Theory Appl* 2016; 11: 1153–1161.
12. Yang Y, Qin S and Jiang P. A modified super-twisting sliding mode control with inner feedback and adaptive gain schedule. *Int J Adapt Control Signal Process* 2017; 31: 398–416.
13. Cerman O and Hušek P. Adaptive fuzzy sliding mode control for electro-hydraulic servo mechanism. *Expert Syst Appl* 2012; 39: 10269–10277.
14. Amieur T, Sedraoui M, Amieur O, et al. Adaptive fuzzy sliding mode control for uncertain nonlinear SISO systems. In: *15th international conference on sciences and techniques of automatic control and computer engineering (STA)* IEEE, Hammamet, Tunisia, 2014, pp.142–147.
15. Zhan L and Zhou K. Adaptive fuzzy sliding mode control for a robotic aircraft flexible tooling system. *Int J Adv Manuf Technol* 2013; 69: 1469–1481.
16. Guan P, Xue L, Liu X-H, et al. The adaptive fuzzy sliding mode control of hypersonic vehicle. In: *10th world congress on intelligent control and automation (WCICA)*. IEEE, Beijing, China, 2012, pp.51–56.
17. Singh SN, Steinberg ML and Page AB. Nonlinear adaptive and sliding mode flight path control of F/A-18 model. *IEEE Trans Aerosp Electron Syst* 2003; 39: 1250–1262.
18. Jia Z, Yu J, Mei Y, et al. Integral backstepping sliding mode control for quadrotor helicopter under external uncertain disturbances. *Aerosp Sci Technol* 2017; 68: 299–307.
19. 771440Su H and Zhang W. A combined backstepping and dynamic surface control to adaptive fuzzy state-feedback control. *Int J Adapt Control Signal Process* 2017; 31: 1666–1685.

20. Yang Y and Yan Y. Attitude regulation for unmanned quadrotors using adaptive fuzzy gain-scheduling sliding mode control. *Aerosp Sci Technol* 2016; 54: 208–217.
21. Norton M, Stojcevski A, Kouzani A, et al. Adaptive fuzzy multi-surface sliding control of multiple-input and multiple-output autonomous flight systems. *IET Control Theory Appl* 2015; 9: 587–597.
22. Rubagotti M, Estrada A, Castanos F, et al. Integral sliding mode control for nonlinear systems with matched and unmatched perturbations. *IEEE Trans Autom Control* 2011; 56: 2699–2704.
23. Rao DV and Sinha NK. A sliding mode controller for aircraft simulated entry into spin. *Aerosp Sci Technol* 2013; 28: 154–163.
24. Guruganesh R, Bandyopadhyay B and Arya H. Robust stabilization of micro aerial vehicles with uncertain actuator nonlinearities. *Int J Micro Air Veh* 2014; 6: 43–62.
25. Liu Y, Yang C and Lu Y. Complex modeling and adaptive sliding control law for mars airplane. *Int J Micro Air Veh* 2014; 6: 73–88.
26. Heller M, David R and Holmberg J. Falling leaf motion suppression in the F/A-18 Hornet with revised flight control software. In: *AIAA aerospace sciences meeting*. No. AIAA-2004-542, Reno, Nevada, 5 - 8 January 2004.
27. Ramezani M and Seyedtabaii S. Optimized fighter aircraft roll stabilizer for better suppression of the falling-leaf. *J Aeronaut, Astronaut Aviat* 2014; 46: 96–101.
28. Bessa WM and Barrêto RSS. Adaptive fuzzy sliding mode control of uncertain nonlinear systems. *SBA* 2010; 21: 117–126.